AMERICAN SOCIETY FOR MICROBIOLOGY | Journal of Bacteriology

Aag Hypoxanthine-DNA Glycosylase Is Synthesized in the Forespore Compartment and Involved in Counteracting the Genotoxic and Mutagenic Effects of Hypoxanthine and Alkylated Bases in DNA during *Bacillus subtilis* Sporulation

Víctor M. Ayala-García,[a] Luz I. Valenzuela-García,[a] Peter Setlow,[b] Mario Pedraza-Reyes[a]

Department of Biology, University of Guanajuato, Guanajuato, Guanajuato, Mexico[a]; Department of Molecular Biology and Biophysics, UConn Health, Farmington, Connecticut, USA[b]

ABSTRACT

Aag from *Bacillus subtilis* has been implicated in *in vitro* removal of hypoxanthine and alkylated bases from DNA. The regulation of expression of *aag* in *B. subtilis* and the resistance to genotoxic agents and mutagenic properties of an Aag-deficient strain were studied here. A strain with a transcriptional *aag-lacZ* fusion expressed low levels of β-galactosidase during growth and early sporulation but exhibited increased transcription during late stages of this developmental process. Notably, *aag-lacZ* expression was higher inside the forespore than in the mother cell compartment, and this expression was abolished in a *sigG*-deficient background, suggesting a forespore-specific mechanism of *aag* transcription. Two additional findings supported this suggestion: (i) expression of an *aag-yfp* fusion was observed in the forespore, and (ii) *in vivo* mapping of the *aag* transcription start site revealed the existence of upstream regulatory sequences possessing homology to σ^G-dependent promoters. In comparison with the wild-type strain, disruption of *aag* significantly reduced survival of sporulating *B. subtilis* cells following nitrous acid or methyl methanesulfonate treatments, and the Rif^r mutation frequency was significantly increased in an *aag* strain. These results suggest that Aag protects the genome of developing *B. subtilis* sporangia from the cytotoxic and genotoxic effects of base deamination and alkylation.

IMPORTANCE

In this study, evidence is presented revealing that *aag*, encoding a DNA glycosylase implicated in processing of hypoxanthine and alkylated DNA bases, exhibits a forespore-specific pattern of gene expression during *B. subtilis* sporulation. Consistent with this spatiotemporal mode of expression, Aag was found to protect the sporulating cells of this microorganism from the noxious and mutagenic effects of base deamination and alkylation.

The integrity of genomes of organisms is constantly compromised by intracellular and extracellular factors that have the potential to generate different base modifications, including, oxidations, alkylations, and deaminations (1). These types of nonbulky genetic insults are detected primarily by specific DNA glycosylases and eliminated through the base excision repair (BER) pathway (2). DNA deamination is a major type of spontaneous genetic damage with which cells must contend (3), and the spontaneous loss of the exocyclic amino groups in cytosine, guanine, and adenine yields the bases uracil, xanthine, and hypoxanthine (HX), respectively (4, 5). HX in DNA is potentially mutagenic, since it can pair not only with thymine but also with cytosine and therefore would result in AT-to-GC transitions after DNA replication (6). Organisms such as *Escherichia coli* and *Saccharomyces cerevisiae* employ the 3-methyladenine DNA glycosylases AlkA and MAG, respectively, to process HX and the modified bases 3-methyladenine, 7-methylguanine, and 7-methyladenine (7, 8). Other enzymes of mammalian origin, which are structurally unrelated to *E. coli* AlkA, include alkyl-adenine-DNA glycosylase (AAG), alkyl-*N*-purine-DNA glycosylase (ANPG), and *N*-methylpurine-DNA glycosylase (MPG) from human, mouse, and rat, respectively, and these also can excise alkylated and deaminated bases from DNA (7, 9–16). The physiological relevance of eliminating the base analog HX from DNA is evidenced by the mutator phenotype exhibited by bacteria and mammals deficient in these glycosylases (6, 17).

Deaminated bases can also be excised from DNA by endonuclease V (EndoV), an endonuclease that hydrolyzes the second phosphodiester bond located at the 3′ end of the modified base, and homologs of such enzymes have been described in bacteria, archaea, and eukaryotes (18–21).

A recent report revealed that *Bacillus subtilis* employs uracil DNA glycosylase (Ung) as well as YwqL, an EndoV homolog, to contend with the mutagenic effects of base deamination (22). However, HX can be processed by another repair protein, termed Aag; this *a*lkyl *a*denine *g*lycosylase is encoded in the genome of *B. subtilis* by *aag* (formerly *yxlJ*), and its product possesses functional

Received 18 August 2016 **Accepted** 28 September 2016

Accepted manuscript posted online 3 October 2016

Citation Ayala-García VM, Valenzuela-García LI, Setlow P, Pedraza-Reyes M. 2016. Aag hypoxanthine-DNA glycosylase is synthesized in the forespore compartment and involved in counteracting the genotoxic and mutagenic effects of hypoxanthine and alkylated bases in DNA during *Bacillus subtilis* sporulation. J Bacteriol 198:3345–3354. doi:10.1128/JB.00625-16.

Editor: T. M. Henkin, Ohio State University

Address correspondence to Mario Pedraza-Reyes, pedrama@ugto.mx.

TABLE 1 *B. subtilis* strains and plasmids used in this study

Strain or plasmid	Genotype or description[a]	Reference or source[b]
Strains		
168	*trpC2* (wild type)	Laboratory stock
WN118	*sigGΔ1 trpC2*	30
PERM791	*ywqL*::*lacZ* Er^r	22
PERM1246	*aag*::*lacZ* Er^r	pPERM1243→168
PERM1286	*aag*::*yfp* Cm^r	pPERM1283→168
PERM1322	*sigGΔ1 trpC2* Δ*aag*::*lacZ* Cm^r	pPERM1318→WN118
PERM1374	*sigGΔ1 trpC2* Δ*aag*::*lacZ* Cm^r (pDG148 [P_{spac}-empty Kan^r])	pDG148→PERM1322
PERM1375	*sigGΔ1 trpC2* Δ*aag*::*lacZ* Cm^r (pDG298 [pDG148::P_{spac}-*sigG* Kan^r])	pDG298→PERM1322
PERM1385	Δ*aag*::*lacZ* Cm^r Δ*ywqL*::*lacZ* Er^r	pPERM1318→PERM791
Plasmids		
pDG148	Shuttle IPTG-inducible P_{spac} vector; Amp^r Kan^r	Laboratory stock
pDG298	pDG148 containing P_{spac}-*sigG* gene; Amp^r Kan^r	30
pMUTIN4	Integrational *lacZ* fusion vector; Amp^r Er^r	28
pMUTIN4cat	Integrational *lacZ* fusion vector; Cm^r	29
pSG1187	Integrational *yfp* fusion vector; Amp^r Cm^r	31
pPERM1243	pMUTIN4 containing an internal region (360 bp) of *aag*; Er^r	This study
pPERM1283	pSG1187 containing the RBS and ORF (606 bp) of *aag*; Amp^r Cm^r	This study
pPERM1318	pMUTIN4cat containing an internal region (360 bp) of *aag*; Er^r	This study

[a] Selection markers: Amp, ampicillin; Cm, chloramphenicol; Er, erythromycin; Kan, kanamycin.
[b] X→Y indicates that strain Y was transformed with DNA from source X.

and structural similarity with human AAG (23). In addition, a biochemical study indicated that the purified Aag protein preferentially eliminates HX from DNA over alkylated bases (23). In the genome of *B. subtilis*, *aag* is oriented adjacent to but in the opposite orientation from *katX*, a gene expressed only in the developing forespore compartment of sporulating cells and encoding a catalase that protects germinating spores against hydrogen peroxide (24). Despite studies reporting induction of *aag* as part of the general stress response (25, 26), inspection of the *katX-aag* intergenic region does not reveal DNA sequences with obvious homology to vegetative or sporulation promoters that may regulate *aag* expression. Therefore, the molecular mechanisms involved in regulating the expression of *aag* during the life cycle of *B. subtilis* were studied in this work. Our results demonstrated a forespore-specific mode of expression of *aag*. In addition, exposure of *B. subtilis* sporulating cells lacking Aag to deaminating and alkylating chemicals resulted in increased mutagenesis and more cell killing than for wild-type cells. We propose that *aag* is expressed during sporulation and that its protein product counteracts the mutagenic effects of hypoxanthine and alkylated bases that may potentially interfere with spore morphogenesis.

MATERIALS AND METHODS

Strain construction and culture conditions. The strains of *B. subtilis* and plasmids used in this work are listed in Table 1 and were constructed using standard molecular biology techniques (27).

To obtain strains harboring a transcriptional *aag-lacZ* fusion, the integrative vector pMUTIN4 (28) or a chloramphenicol-resistant variant of this plasmid, pMUTIN4cat (29), was utilized. For recombinant plasmid construction, a 360-bp HindIII/BamHI internal fragment of *aag* (positions +121 to + 480 relative to the *aag* start codon) was amplified by PCR using chromosomal DNA of *B. subtilis* 168 and Vent DNA polymerase (New England BioLabs, Ipswich, MA). The oligonucleotide primers used for the amplification of the *aag* fragment were 5′-GCAAGCTTTATATT GTGGAAACAGAGG (forward) and 5′-GCGGATCCGTACCCGCTTTC GATGTAA (reverse), including the restriction sites (underlined) for cloning the amplified *aag* product between the HindIII/BamHI sites of pMUTIN4 or pMUTIN4cat. The resulting constructs, termed pPERM1243 (*aag*::*lacZ*, obtained in pMUTIN4) and pPERM1318 (*aag*::*lacZ*, obtained in pMUTIN4cat) were propagated in *E. coli* XL10-Gold cells (Stratagene, La Jolla, CA). Plasmid pPERM1243 was used to transform competent cells of *B. subtilis* 168, generating strain PERM1246 (*aag-lacZ*), and plasmid pPERM1318 was used to transform competent cells of *B. subtilis* WN118 (*sigGΔ1 trpC2*) (30), generating strain PERM1322 (*sigGΔ1 trpC2 aag-lacZ*). The correct integration of the constructions into the *aag* locus was corroborated by PCR using specific oligonucleotide primers (data not shown).

To investigate the subcellular localization of Aag during sporulation, a translational *aag*::*yfp* fusion was constructed by employing the integrative plasmid pSG1187 (31). In this construction, a 606-bp-long KpnI/ClaI fragment of *aag* (positions −18 to +588 relative to the *aag* start codon) including the entire open reading frame (ORF) and the ribosome binding site (RBS) of the *aag* gene was amplified by PCR using chromosomal DNA of *B. subtilis* 168. The oligonucleotide primers used for the amplification of this *aag* fragment were 5′-GCGGTACCAAAAGGAGAGGTCGATT CGTG (forward) and 5′-GCATCGATCGACACGTACCTGTTTCCCGT (reverse), including the restriction sites (underlined) for cloning the amplified products of *aag* between the KpnI/ClaI sites of pSG1187. The resulting construct, designated pPERM1283 (*aag*::*yfp*), was propagated in *E. coli* GM161 cells. This plasmid was used to transform competent cells of *B. subtilis* strain 168, generating strain PERM1286 (*aag-yfp*). The correct integration of constructions into the corresponding *aag* locus was verified by PCR using specific oligonucleotide primers (data not shown).

To complement the σ^G deficiency of *B. subtilis* strain PERM1322 bearing a chromosomal copy of the *aag-lacZ* fusion, plasmid pDG298 (30), carrying a copy of *sigG* under the control of the IPTG (isopropyl-β-D-thiogalactopyranoside)-inducible P_{spac} promoter in plasmid pDG148, was transformed into competent cells of *B. subtilis* PERM1322, generating strain PERM1375 [*sigGΔ1 trpC2 aag-lacZ*(pDG298, pDG148::P_{spac}-*sigG*)]. As a control, the empty pDG148 vector (P_{spac}-empty) was also used to transform strain PERM1322, generating strain PERM1374 [*sigGΔ1 trpC2 aag-lacZ*(pDG148::P_{spac}-empty)]. The *aag ywqL* strain (PERM1385) was obtained by transformation of the *ywqL* strain (PERM791) (22) with pPERM1318.

Liquid cultures of *B. subtilis* were grown in Luria-Bertani (LB) medium, Difco antibiotic no. 3 (PAB) medium, or Difco sporulation medium (DSM) (32). When required, erythromycin (Er) (5 μg ml^{-1}), chlor-

amphenicol (Cm) (5 μg ml^{-1}), kanamycin (Kn) (10 μg ml^{-1}), or IPTG (1 mM) was added to media. *E. coli* cultures were grown in LB medium supplemented with ampicillin (Amp) (100 μg ml^{-1}) or Cm (25 μg ml^{-1}). Solid media were obtained by adding bacteriology agar (15 g liter^{-1}) to the liquid media. For all experiments, strains were grown overnight in liquid LB medium at 37°C and then diluted 100-fold into appropriate medium. All liquid cultures were incubated at 37°C with vigorous aeration. Cultures on solid media were incubated at 37°C in the dark.

β-Galactosidase assay. All *B. subtilis* strains harboring the *aag-lacZ* fusion were grown in either liquid PAB medium (to avoid sporulation) or liquid DSM (to promote sporulation) at 37°C. Cells from 1-ml samples were harvested by centrifugation during vegetative growth and throughout sporulation when appropriate. Cell pellets were immediately frozen and stored at −20°C prior to determination of β-galactosidase activity as previously described (33). The level of β-galactosidase during sporulation was determined as follows. Cells collected from the different sporulation stages were treated with lysozyme and centrifuged (14,500 × *g*, 2 min), and β-galactosidase in the supernatant was assayed using *ortho*-nitrophenyl-β-D-galactopyranoside (ONPG) as the substrate, and this value was assigned to the mother cell fraction. The pellet fraction (lysozyme-resistant forespores containing spore coats) from sporulation stages T_4 (4 h after the onset of sporulation) to T_8 was subjected to spore coat removal (33), washed five times with TS buffer (25 mM Tris-HCl [pH 7.4], 0.1 M NaCl), and subjected to lysozyme treatment, and the β-galactosidase assay was repeated to determine the β-galactosidase activity inside forespores. The β-galactosidase activity was expressed in Miller units (34). The endogenous ONPGase-specific activity expressed by the wild-type strain without a *lacZ* fusion during growth and sporulation was determined in parallel and subtracted from the data obtained for strains carrying the *aag-lacZ* fusion. This correction was at most ~2 Miller units.

Microscopy. *B. subtilis* containing the *aag*::*yfp* fusion was sporulated in DSM. FM4-64 (5 μg ml^{-1}) was added to sporulating cells at stage T_1 to stain membranes. At the appropriate times, samples of 0.5 ml of the culture were harvested by centrifugation (14,500 × *g*, 1 min) and resuspended in 50 μl of fresh DSM. Cells from 5 μl of this concentrated cell suspension were immobilized on an agarose spot (20 mg ml^{-1}) placed on a microscopy slide and covered with a coverslip prior to microscopic analysis. Fluorescence microscopy was performed with a Zeiss Axioscope A1 microscope equipped with an AxioCam ICc1. Images were acquired and adjusted only for brightness and contrast with the AxioVision V 4.8.2 software. Exposure times were typically 2 s for Aag-yellow fluorescent protein (Aag-YFP) and 0.5 s for FM4-64. Samples of the wild-type parental strain were collected at the same stages of the sporulation process as described for the strain carrying the *aag*::*yfp* fusion and processed for microscopic analysis. No fluorescent background corresponding to the YFP channel was detected in the sporangia analyzed (results not shown).

Primer extension. The 5′ end of *aag* mRNA was mapped by primer extension of *aag* transcripts produced during wild-type *B. subtilis* sporulation or following induction of *sigG* expression during logarithmic growth of strain PERM1375 as follows. Samples of total RNA (40 μg), isolated as previously described (35), were hybridized with the 20-mer oligonucleotide 5′-TAGCCTGACGCTGTGCCTTC-3′, which was complementary to the *aag* mRNA from nucleotide +103 to +122 relative to the translational start codon of *aag*. The oligonucleotide primer was radiolabeled on its 5′ end with [γ-^{32}P]ATP (PerkinElmer, Foster City, CA) and T4 polynucleotide kinase (New England BioLabs, Ipswich, MA), and the primer was extended with 40 units of Moloney murine leukemia virus (M-MLV) RNase H Minus reverse transcriptase (Promega, Madison, WI). The position of the extension product was determined by running a DNA sequencing reaction generated with the same 20-nucleotide (nt) primer and a 1-kb PCR product extending from bp −412 to +588 relative to the *aag* start codon using a Thermo Sequenase dye primer manual cycle sequencing kit (Affymetrix-USB, Cleveland, OH). The extension products and the sequencing DNA ladder were separated by electrophoresis through an 8 M urea–6% polyacrylamide DNA sequencing gel and analyzed using a personal molecular imager (Bio-Rad Laboratories, Hercules, CA) and Quantity-One software.

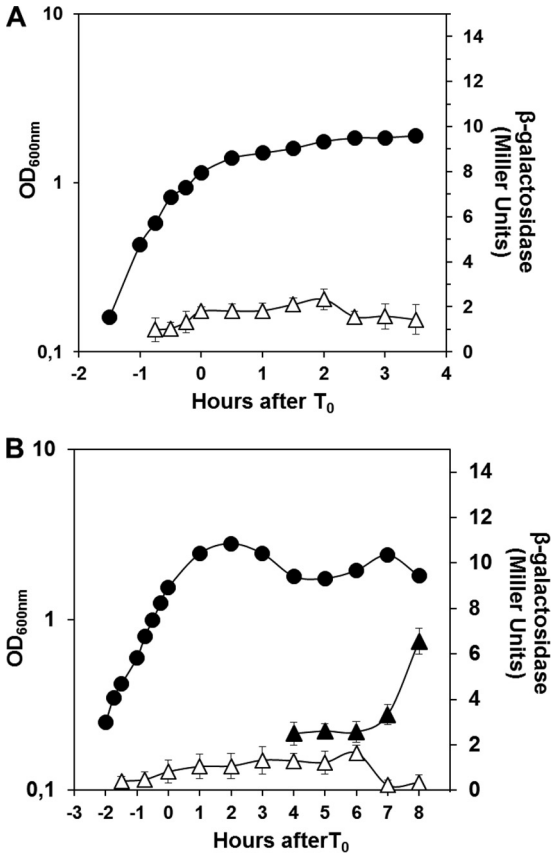

FIG 1 Expression of *aag* during *B. subtilis* growth and sporulation. (A) β-Galactosidase activity from an *aag-lacZ* fusion during vegetative growth. *B. subtilis* strain PERM1246 harboring an *aag-lacZ* fusion was grown in PAB medium and the OD_{600} measured (●). Cells were collected at various times, and the β-galactosidase activity of growing cells (△) was determined as described in Materials and Methods. Values for β-galactosidase specific activity are the averages of values from three independent experiments ± standard deviations (SD). (B) β-Galactosidase specific activity from an *aag-lacZ* fusion during sporulation. *B. subtilis* strain PERM1246 harboring an *aag-lacZ* fusion was induced to sporulate in DSM and the OD_{600} measured (●). Time zero of sporulation (T_0) is defined as the time when log-phase cell growth stops. Cells were collected at various times, and β-galactosidase assays were conducted in both mother cell (△) and forespore (▲) fractions as described in Materials and Methods. Values for β-galactosidase specific activity are the averages of values from three independent experiments ± SD.

Determination of sporangial sensitivity to HNO_2 and MMS. The sensitivity of *B. subtilis* sporulating cells to HNO_2 or methyl methanesulfonate (MMS) was determined from dose-response curves for the wild-type strain and the *aag*, *ywqL*, and *aag ywqL* strains. Cells of various strains were sporulated in liquid DSM, collected by centrifugation (5,000 × *g*, 10 min) at 4.5 h after the onset of sporulation ($T_{4.5}$, with T_0 the time when exponential growth of cultures stopped), washed twice with phosphate-buffered saline (PBS) (0.7% Na_2HPO_4, 0.3% KH_2PO_4, 0.4% NaCl [pH 7.5]), and adjusted to an optical density at 600 nm (OD_{600}) of 1.0. Two-milliliter samples of cellular suspension were treated with different concentrations of either HNO_2 (0, 2.5, 5, or 7.5 mM), prepared as was previously described (36), or MMS (0, 30, 60, or 90 mM) and incubated for 1 h at room temperature with shaking. After treatment, cells were washed again with PBS, and cell viability was determined by plating aliquots of serial dilutions on LB agar plates that were incubated overnight at 37°C and counting colonies.

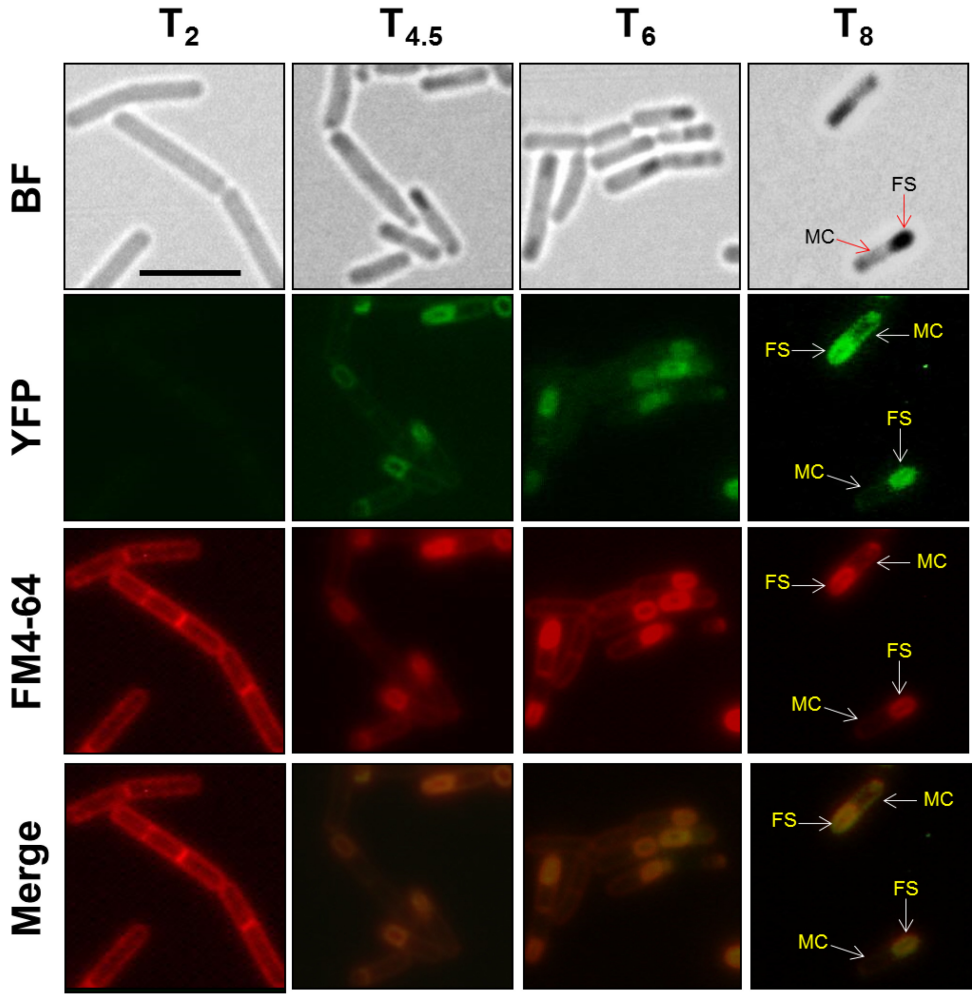

FIG 2 Localization of Aag-YFP during *B. subtilis* sporulation. *B. subtilis* strain PERM1286 harboring a translational in-frame *aag-yfp* fusion was grown and sporulated in DSM. At 2, 4.5, 6, and 8 h after the onset of sporulation, sporulating cells were analyzed by bright-field (BF) and fluorescence (YFP and FM4-64) microscopy as described in Materials and Methods. Overlain images of YFP and FM4-64 at each time point are depicted as merge. MC, mother cell; FS, forespore compartments. Scale bar, 5 μM.

Two-milliliter aliquots of $T_{4.5}$ sporulating cells of all strains adjusted to an OD_{600} of 1.0 were treated for 1 h at room temperature with the 50% lethal dose (LD_{50}) of HNO_2 or MMS calculated for wild-type cells and washed twice with PBS, and 10-fold serial dilutions were spot plated on solid LB medium. The plates were incubated overnight at 37°C and then photographed in a Gel-Doc EZ imaging system (Bio-Rad Laboratories, Hercules, CA).

Determination of HNO_2- or MMS-induced mutagenesis. Cells of different strains were sporulated in liquid DSM and collected by centrifugation (5,000 × *g*, 10 min) at stage $T_{4.5}$, and each culture was divided in half and washed with PBS. One of the cultures was untreated, and the other was treated for 1 h at room temperature with the LD_{50} of either HNO_2 or MMS (calculated for each strain from the survival curves in Fig. 6A and 7A). Mutation frequencies were calculated by plating aliquots on six LB plates containing 10 μg ml^{-1} of rifampin (Rif) as well as plating aliquots of the appropriate dilution on LB plates to determine the total viable count. Rif^r colonies were counted after 48 h of incubation at 37°C.

Statistical analyses. Differences between lethal doses obtained from survival curves for HNO_2 and MMS treatments were calculated by performing one-way analysis of variance (ANOVA) followed by Tukey's *post hoc* analyses, with a *P* value of <0.05 considered significant. For HNO_2- or MMS-induced mutagenesis, results were tested by the Mann-Whitney U test, and analyses were done using Minitab17 software.

RESULTS

Expression of *aag* is primarily during spore development. To analyze the expression of *aag* during the life cycle of *B. subtilis*, a recombinant strain bearing a transcriptional in-frame *aag-lacZ* fusion (PERM1246) was inoculated in liquid PAB medium to promote vegetative growth. Under these conditions, *aag*-directed β-galactosidase activity was very low during exponential growth and stationary phase (Fig. 1A). This *aag-lacZ* fusion was also used to measure *aag* expression during the differentiation process of sporulation. Cells of strain PERM1246 were sporulated in liquid DSM, and samples harvested at various times during growth and sporulation were assayed for β-galactosidase. These assays showed low levels of expression of the reporter gene during exponential growth and early sporulation (Fig. 1B). Cell fractionation experiments with cell samples collected from sporulation stages T_4 to T_8 revealed that whereas β-galactosidase activity from the *aag-lacZ* fusion decreased in the mother cell compartment, the levels of this enzyme activity increased significantly in the forespore fraction (Fig. 1B). Together these results suggest that *aag* is expressed primarily during sporulation and in the forespore compartment of the sporulating cell.

Expression of a chimeric Aag-YFP protein occurs mainly inside the forespore compartment. To further confirm the forespore-specific transcription of *aag*, we analyzed the compartmental synthesis of a chimeric Aag-YFP protein during sporulation of a *B. subtilis* strain bearing a translational in-frame *aag-yfp* fusion in the *aag* locus (PERM1286). Samples of sporulating cells stained with FM4-64, a lipophilic dye that strongly adheres to the cell membrane and allows discernment of both compartments of sporangia (mother cell and forespore), were collected from stages T_2, $T_{4.5}$, T_6, and T_8 of sporulation. Each sample was examined by epifluorescence microscopy. The results revealed that the Aag-YFP protein was present in the forespore compartment but absent from the mother cell compartment (Fig. 2). These results further support the concept that *aag* is transcribed in the forespore compartment during late stages of sporulation.

Expression of *aag* is dependent on the forespore-specific sigma factor σ^G. The forespore-specific pattern of expression exhibited by *aag* was reminiscent of a group of genes, the σ^G regulon, that are transcribed during late stages of sporulation exclusively in the forespore compartment by RNA polymerase with the forespore-specific sigma factor σ^G (37, 38). To investigate whether *aag* expression was indeed dependent on σ^G, the transcriptional *aag-lacZ* fusion was inserted into the *aag* locus of a *B. subtilis* Δ*sigG* strain (WN118) (30) by homologous recombination. The resulting strain (*B. subtilis* PERM1322) was sporulated in liquid DSM, and the *aag*-directed β-galactosidase activity was determined from various samples collected during growth and sporulation. Notably, expression of the *aag-lacZ* fusion was almost completely abolished inside the forespore compartment in the Δ*sigG* genetic background (Fig. 3A), strongly suggesting that *aag* transcription is σ^G dependent. To further test this suggestion, strain PERM1322 was transformed with the self-replicating plasmid pDG298 harboring a copy of *sigG* under the control of an IPTG-inducible P*spac* promoter (30), giving strain PERM1375. As a control, strain PERM1322 was also transformed with plasmid pDG148 (empty vector), generating strain PERM1374. Both the PERM1374 and PERM1375 strains were grown in PAB medium to an OD_{600} of 0.5, and IPTG was added to 1 mM. As shown in Fig. 3B, the addition of IPTG induced the expression of the *aag-lacZ* fusion in the strain that contained the P*spac-sigG* cassette but not in the control strain bearing the empty vector pDG148.

Mapping the 5′ ends of *aag* mRNA. The genetic arrangement of the *aag* locus reveals that this gene is preceded by *katX*, encoding the major catalase in dormant spores and transcribed divergently with respect to *aag* (Fig. 4A) (24), and followed by *yxzF*, which codes for an uncharacterized protein. The *aag* and *yxzF* genes are separated by only 28 bp, and there is not an apparent transcriptional terminator in this intergenic region, suggesting that these two genes are in a bicistronic operon (Fig. 4A). As demonstrated in this work, the expression of *aag* was dependent on the forespore-specific sigma factor σ^G. Therefore, the likely promoter sequence recognized by σ^G to activate *aag* transcription was located by mapping the 5′ end of *aag* mRNA produced *in vivo*. Total RNA isolated from the wild-type strain during stage T_5 of sporulation as well as from vegetative cells of PERM1375, 3 h after IPTG induction of *sigG*, was hybridized with a 19-nt-long radioactive primer complementary to *aag* mRNA from nt +103 to +122 relative to the *aag* translational start codon and subjected to primer extension analysis. This analysis revealed the synthesis of an extension product beginning 69 bp upstream of the *aag* translation start codon using mRNAs from either sporulating cells of the wild-type strain or vegetative cells of the strain overexpressing *sigG* (Fig. 4B, lanes 1 and 2).

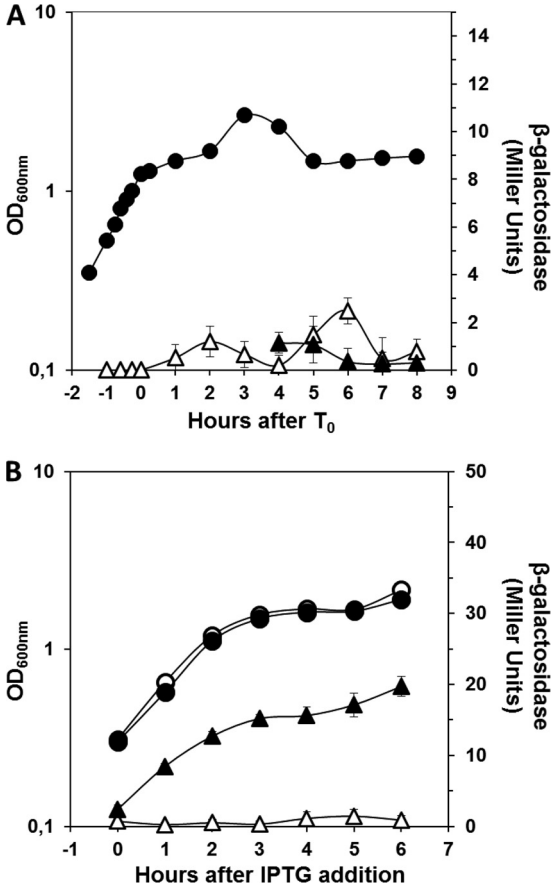

FIG 3 σ^G dependence of *aag-lacZ* expression. (A) β-Galactosidase activity of *aag-lacZ* during sporulation of the Δ*sigG* strain. *B. subtilis* strain PERM1375 harboring an *aag-lacZ* fusion in a Δ*sigG* genetic background was sporulated in DSM and the OD_{600} measured (●). Cells were collected at various times, and β-galactosidase activity was assayed in mother cell (△) and forespore (▲) fractions as described in Materials and Methods. Values for β-galactosidase specific activity are the averages of values from three independent experiments ± SD. (B) β-Galactosidase activity from an *aag-lacZ* fusion induced by overexpression of *sigG* during vegetative growth. *B. subtilis* strains PERM1375 and PERM1374 harboring an *aag-lacZ* fusion in a Δ*sigG* genetic background containing either a P_{spac}::*sigG* gene fusion (●) or the empty vector (○) were grown in PAB medium and induced with IPTG (1 mM) when an OD_{600} of 0.5 was reached. The OD_{600}s of cultures were measured (● and ○), cells were collected at various times, and β-galactosidase assays from cells that were (▲) or were not (△) complemented with *sigG* were conducted as described in Materials and Methods. Values for β-galactosidase specific activity are the averages of values from three independent experiments ± SD.

Having found that an adenine located 69 nt upstream of the first codon of the *aag* ORF functions as the transcription start for the synthesis of *aag* mRNAs, we inspected the sequences preceding this site to identify possible σ^G promoter sequences (39). Notably, regions located at −10 and −35 with respect to the transcription start site, and separated by 18 nt, exhibited a good level of homology with the consensus −10 and −35 regions of σ^G-dependent promoters (Fig. 5).

Aag and YwqL protect sporulating *B. subtilis* cells from cytotoxic and genotoxic effects of HNO_2. The forespore-specific

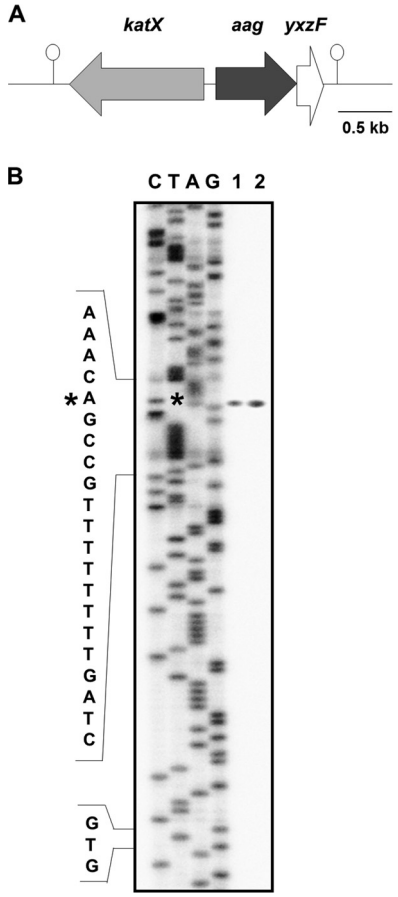

FIG 4 Genetic map of the *aag* region and mapping of the *aag* promoter. (A) The *B. subtilis* chromosomal region around *aag*. The *katX* gene is divergently transcribed upstream of *aag*, and *aag* and *yxzF* may comprise a bicistronic operon. Hairpin structures denote putative transcriptional terminators. The drawing is to scale. (B) Primer extension analysis to identify the 5′ end of *aag* mRNA. Total RNA was isolated from T_6 sporulating cells of *B. subtilis* strain 168 (wild type) grown in DSM (lane 1) or vegetative cells of strain PERM1375 grown in PAB medium, induced with IPTG, and harvested 3 h after IPTG addition (lane 2). Primer extension was performed as described in Materials and Methods. The asterisk indicates the position of the primer extension product relative to the DNA sequencing ladder (lanes C, T, A, and G). The position of the mapped 5′ end of *aag* mRNA is denoted with an asterisk. "GTG" indicates the position of the *aag* translation start codon.

expression exhibited by *aag* prompted us to investigate the DNA repair functions of Aag during *B. subtilis* spore development. To this end, sporangia from wild-type and *aag* strains collected at $T_{4.5}$ of sporulation were challenged with increasing doses of nitrous acid (HNO_2), an agent that promotes deamination of adenine to HX (40). Notably, the Aag-deficient sporangia were only slightly more susceptible to the genotoxic effects of HNO_2 than sporangia from the parental wild-type strain (Fig. 6), although the LD_{90} values for HNO_2 were significantly different between wild-type and *aag* sporangia (Table 2). The relatively small differences seen in the latter experiment suggested the existence of additional pathways involved in counteracting HNO_2-induced base deamination in these sporulating cells. In agreement with this notion, disruption of *ywqL*, encoding an endonuclease capable of processing a wider range of deaminated bases (22; V. M. Ayala-Garcia and M. Pedraza-Reyes, unpublished data), generated sporangia that were

σ^G-dependent promoter consensus sequence:

```
------GHATR-------18nt---------CATXHTA-------
      -35                      -10
```

P*aag* sequence:

```
GAACGGTAACAATATTCCCTGAATGGAAAGATTTTAAACAGC
      -35                      -10
```

FIG 5 Comparison of the consensus σ^G (39) promoter sequence with the putative promoter sequences (P*aag*) upstream of the *aag* ORF. Perfect matches are in bold. The position of the *aag* transcription start site is denoted with an asterisk. Abbreviations: H, A or C; R, A or G; and X, A or T.

significantly more sensitive to HNO_2 than those of the Aag-deficient strain (Fig. 6; Table 2). Importantly, disruption of *aag* did not significantly increase the sensitivity of the *ywqL* sporangia to the genotoxic effects of HNO_2 (Fig. 6; Table 2). Together, these results suggest that YwqL rather than Aag is most important in eliminating HX and probably other deaminated bases from DNA during *B. subtilis* sporulation.

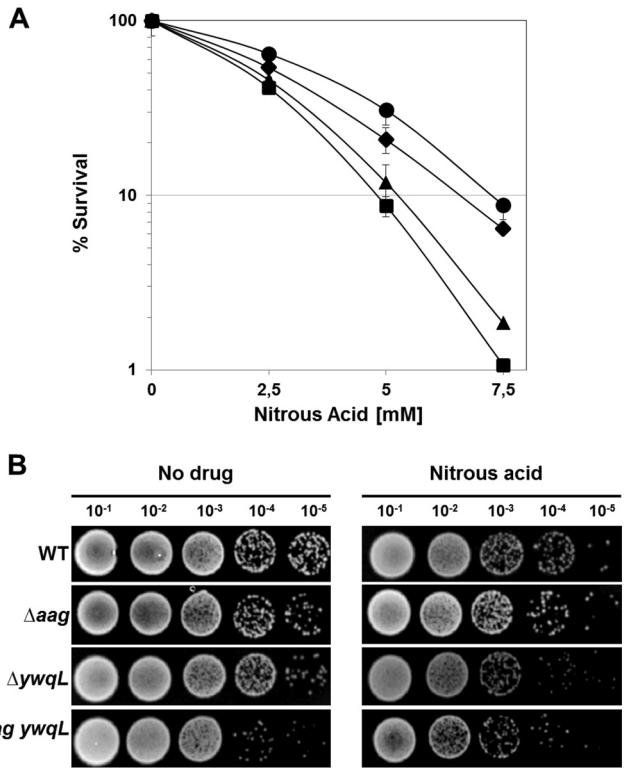

FIG 6 Sensitivity of sporulating cells to HNO_2. (A) Survival of *B. subtilis* wild-type (●), *aag* (◆), *ywqL* (▲), and *aag ywqL* (■) strains following HNO_2 treatment. Cells from various strains were sporulated in liquid DSM and treated with different concentrations of HNO_2 at 4.5 h after the onset of sporulation, and cell viability was determined as described in Materials and Methods. Results are expressed as averages ± SD from at least three independent experiments. (B) Resistance of *B. subtilis* wild-type (WT), *aag*, *ywqL*, and *aag ywqL* strains after exposure to HNO_2. Cells from all strains were sporulated in liquid DSM, treated with the LD_{50} of HNO_2 (calculated from the dose-response curve in panel A for the wild-type strain) at 4.5 h after the onset of sporulation, spot plated, grown, and photographed as described in Materials and Methods.

TABLE 2 LD_{50} and LD_{90} values for wild-type and mutant sporulating cells treated with HNO_2 and MMS

Strain	HNO_2		MMS	
	LD_{50} (mM)[a]	LD_{90} (mM)	LD_{50} (mM)	LD_{90} (mM)
WT	3.47 ± 0.11 a	7.49 ± 0.06 a	38.86 ± 0.30 a	71.20 ± 0.57 a
PERM1246 (*aag*)	2.92 ± 0.05 a	6.82 ± 0.09 b	15.16 ± 0.17 b	32.69 ± 0.37 b
PERM791 (*ywqL*)	2.17 ± 0.09 b	5.14 ± 0.10 c	37.93 ± 0.61 a	69.49 ± 0.67 a
PERM1385 (*aag ywqL*)	1.90 ± 0.06 b	4.80 ± 0.08 c	14.94 ± 0.31 b	32.47 ± 0.40 b

[a] Values are means ± standard errors of the means (SEM). Letters indicate statistically significantly different values between strains as determined by one-way analysis of variance (ANOVA) followed by Tukey's *post hoc* tests ($P < 0.05$).

Aag protects sporulating *B. subtilis* cells from cytotoxic and genotoxic effects of MMS. In addition to processing HX, Aag also can remove 3-mA and 3-mG from DNA (23). Therefore, we compared the abilities of wild-type and mutant sporangia lacking Aag and/or YwqL to survive treatment with the alkylating agent MMS. Interestingly, the absence of Aag but not YwqL sensitized sporulating cells to the genotoxic effects of MMS, and this effect did not increase in cells deficient for both repair proteins (Fig. 7; Table 2). Taken together, these results suggest that Aag is primarily involved in eliminating alkylated DNA bases during spore development.

Aag and YwqL counteract the mutagenic effects of HNO_2 and MMS. We next investigated whether Aag and/or YwqL was involved in preventing the mutagenic effects promoted by HNO_2 and MMS during spore development. To this end, sporulating *B. subtilis* wild-type, *aag*, *ywqL*, and *aag ywqL* cells at $T_{4.5}$ were treated or not with the LD_{50} of HNO_2 or MMS, and the mutation frequency for colonies resistant to rifampin (Rif^r) was determined for each strain. With respect to wild-type sporulating cells, the lack of Aag or YwqL alone did not increase the spontaneous Rif^r mutation frequency. However, this parameter increased significantly when both *aag* and *ywqL* were absent (Fig. 8). HNO_2 treatment increased mutagenesis in sporangia of all the strains tested, but the effect was maximal in strains that were deficient for either Aag or YwqL and did not increase in *aag ywqL* sporangia (Fig. 8A). In contrast, MMS had a large mutagenic effect on sporulating cells of the *aag* and *aag ywqL* strains but not those of the *ywqL* strain (Fig. 8B). Overall, Aag and YwqL both seem to participate in counteracting the mutagenic effects promoted by factors that damage the DNA of sporulating cells through deamination and alkylation of bases.

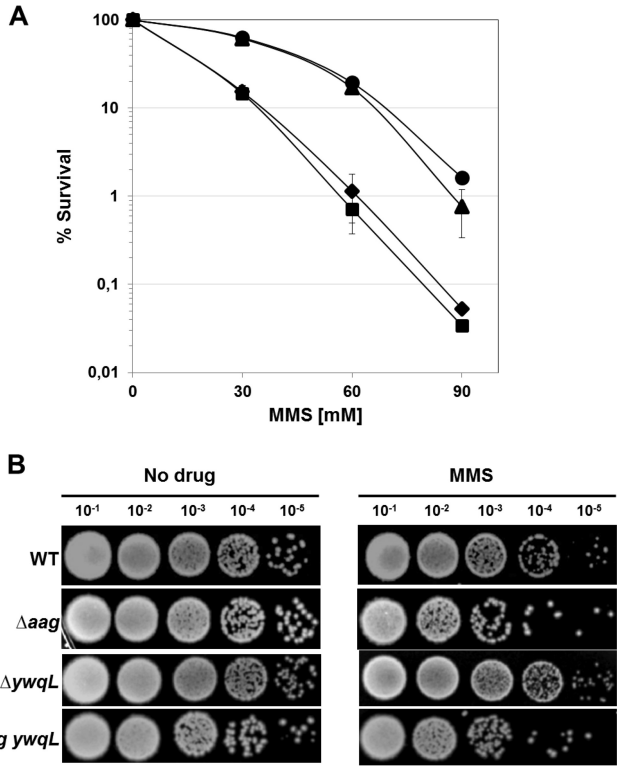

FIG 7 Sensitivity of sporulating cells to MMS. (A) Killing of *B. subtilis* wild-type (●), *aag* (◆), *ywqL* (▲), and *aag ywqL* (■) strains by MMS. Cells from all strains were sporulated in liquid DSM and treated with different concentrations of MMS at 4.5 h after the onset of sporulation, and cell viability was determined as described in Materials and Methods. Results are expressed as averages ± SD from at least three independent experiments. (B) Resistance of *B. subtilis* wild-type (WT), *aag*, *ywqL*, and *aag ywqL* strains after exposure to MMS. Cells from all strains were sporulated in liquid DSM, treated with the LD_{50} of MMS (calculated from the dose-response curve in panel A for the wild-type strain) at 4.5 h after the onset of sporulation, spot plated, grown, and photographed as described in Materials and Methods.

DISCUSSION

The soil bacterium *B. subtilis* may be exposed to a plethora of environmental pollutants, including reactive nitrogen species (RNS) generated by oxidation or reduction of nitric oxide (NO·). RNS resulting from microbial denitrification (41) include nitrogen dioxide (NO_2·), peroxynitrite ($ONOO^-$), and peroxynitrous acid (ONOOH) (42), all of which are potent triggers of DNA base deamination, generating, among others, the base analog HX (40). In vegetative cells of *B. subtilis*, HX may potentially be removed from DNA by the endonuclease YwqL (22). However, this organism also possesses *aag*, encoding a DNA glycosylase that operates on HX as well as alkylated adenine derivatives (23).

In contrast to *alkA*, *B. subtilis aag* does not seem to be under the control of the Ada response (43); however, *aag* expression is regulated in concert with the general stress σ^B regulon (25, 26). Furthermore, inducible levels of expression of this gene were detected during spore germination/outgrowth (44). Our analysis using a *B. subtilis* strain carrying a transcriptional *aag-lacZ* fusion revealed that *aag* transcription is very low during exponential growth and early stages of sporulation but increases significantly during late stages of this developmental process. Of note, genes encoding a number of DNA repair proteins, including *splB*, *ywjD*, *mfd*, *uvrA*, and *recA*, exhibit similar expression patterns (45–48). In addition, results from one transcriptomic study did report *aag* expression associated with sporulation stages T_7 and T_8 (49). In the current work, results from fractionation of sporulating cells of the *aag-lacZ* strain and microscopic analysis of sporangia carrying an *aag-yfp* gene fusion provided strong evidence that transcription of *aag*

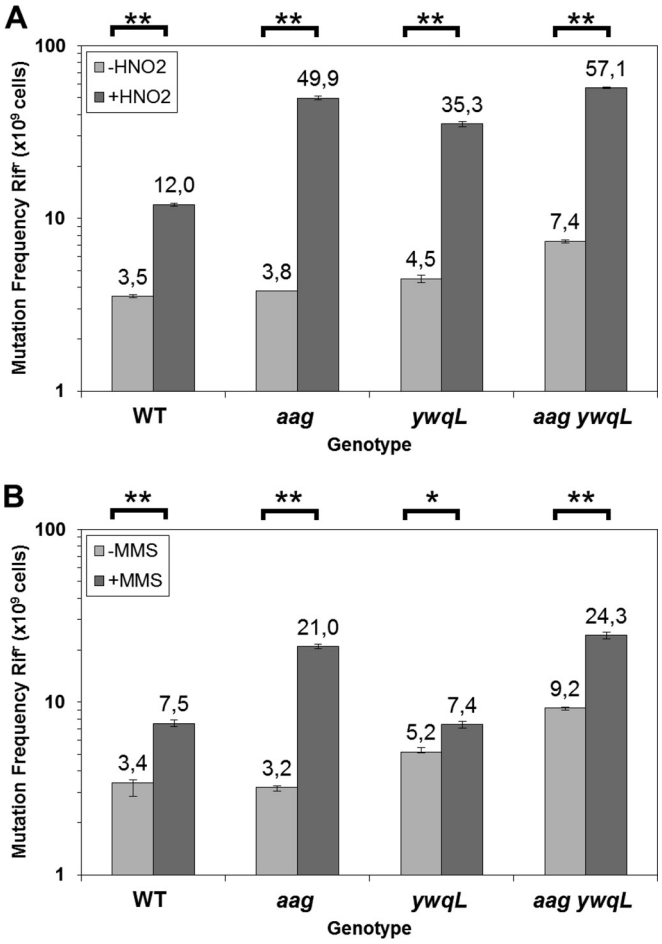

FIG 8 Frequencies of mutation to Rif^r. Cells of *B. subtilis* wild-type, *aag*, *ywqL*, and *aag ywqL* strains were sporulated in liquid DSM and treated with the LD_{50} for each strain of either HNO_2 (A) or MMS (B) at 4.5 h after the onset of sporulation. The levels of Rif^r cells with (+) or without (−) treatment exposure were determined. Each bar represents the mean of data collected from three independent experiments, and error bars represent the standard error of the mean (SEM). *, $P < 0.05$; **, $P < 0.01$ (by the Mann-Whitney U test).

takes place mainly in the forespore compartment of *B. subtilis* sporangia. Furthermore, genetic evidence showing that expression of *aag-lacZ* was eliminated in a σ^G-deficient strain and restored by in *trans* expression of σ^G strongly supports the notion that *aag* is expressed in the forespore compartment under the control of RNA polymerase with σ^G. Based on an *in silico* analysis, a previous report proposed that common regulatory elements may direct the expression of the *katX* and *aag* genes (23). However, primer extension analysis detected specific regulatory regions directing *aag* that are different from those described for *katX* (24). Indeed, the localization of the 5′ end of *aag* mRNA allowed the identification of DNA sequences centered at −10 and −35 relative to the transcription start site that exhibited a reasonable level of homology to −10 and −35 sequences of σ^G-dependent promoters (39). Based on these results, we postulate that *aag* is an additional member of the σ^G regulon. Of note, *katX* was also reported to be part of the σ^B regulon (25, 26), and previous work also demonstrated that σ^F directs *katX* expression inside the forespore compartment during *B. subtilis* sporulation (24).

In agreement with the forespore-specific expression of *aag*, *B. subtilis aag* sporangia exhibited slight but significantly increased susceptibility to HNO_2; however, sporangia deficient for the endonuclease YwqL were more severely sensitized to this genotoxic chemical. These results are in agreement with the ability of YwqL to process the full range of deaminated bases generated by nitrous acid (V. M. Ayala-García and M. Pedraza-Reyes, unpublished data), while Aag acts specifically on HX (23). Interestingly, these two DNA repair proteins played equivalent roles in counteracting the mutagenic effects of HNO_2, since compared to the wild-type strain, the *aag* and *ywqL* strains exhibited higher but almost identical levels of HNO_2-induced mutagenesis. Therefore, Aag and YwqL may work together to protect sporulating cells of *B. subtilis* from the genotoxic, cytotoxic, and mutagenic effects of base deamination.

In a marked contrast, *aag* but not *ywqL* sporangia exhibited increased sensitivity to the alkylating agent MMS. This alkylating agent also induced mutagenesis in the *aag* sporangia but not in *ywqL* sporangia, confirming that YwqL does not act on alkylated DNA. Interestingly, although *B. subtilis* possesses additional pathways to process alkylated bases, including AlkA and the products of the *adaA-adaB* operon (50–53), our results showed that the absence of Aag alone generated sporangia that were more susceptible to the cytotoxic and mutagenic effects of MMS. However, the following observations may explain the latter, somewhat anomalous results: (i) MMS mainly induces the formation of the non-bulky DNA lesions 3-mA, 3-mG, and 7-mG (54, 55), while (ii) the products of the *adaA-adaB* operon and AlkA are more important in removing bulky alkylated lesions generated by *N*-methyl-*N*′-nitro-*N*-nitrosoguanidine (MNNG) and *N*-propyl-*N*′-nitro-*N*-nitrosoguanidine (PNNG) (43).

Finally, as shown in this work, the synthesis of a chimeric Aag-Yfp protein took place inside the forespore compartment, strongly suggesting that Aag is packaged in the dormant spores putatively to eliminate alkylated DNA during spore germination/outgrowth. Indeed, *B. subtilis* spores are not resistant to the genotoxic effects of alkylating agents like MMS (56). Therefore, experiments are under way to explore the contribution of Aag in ensuring the successful return to life of *B. subtilis* spores.

ACKNOWLEDGMENTS

V.M.A.-G. and L.I.V.-G. were supported by a scholarship from the Consejo Nacional de Ciencia y Tecnología (CONACYT).

We are grateful for the excellent technical assistance of Rocío del C. Barajas-Ornelas and Fernando H. Ramírez-Guadiana.

FUNDING INFORMATION

This work, including the efforts of Mario Pedraza-Reyes, was funded by CONACYT (221231 and 205744). This work, including the efforts of Mario Pedraza-Reyes, was funded by University of Guanajuato (936-2016 and 1090-2016).

REFERENCES

1. **Friedberg EC, Walker GC, Siede W, Wood RD, Schultz RA, Ellenberger T.** 2006. DNA repair and mutagenesis, 2nd ed. American Society for Microbiology, Washington, DC.
2. **Dalhus B, Laerdahl JK, Backe PH, Bjørås M.** 2009. DNA base repair—recognition and initiation of catalysis. FEMS Microbiol Rev **33:**1044–1078. http://dx.doi.org/10.1111/j.1574-6976.2009.00188.x.
3. **Yonekura SI, Nakamura N, Yonei S, Zhang-Akiyama QM.** 2009. Generation, biological consequences and repair mechanisms of cytosine

deamination in DNA. J Radiat Res **50:**19–26. http://dx.doi.org/10.1269/jrr.08080.
4. **Lindahl T.** 1993. Instability and decay of the primary structure of DNA. Nature **362:**709–715. http://dx.doi.org/10.1038/362709a0.
5. **Barnes DE, Lindahl T.** 2004. Repair and genetic consequences of endogenous DNA base damage in mammalian cells. Annu Rev Genet **38:**445–476. http://dx.doi.org/10.1146/annurev.genet.38.072902.092448.
6. **Hill-Perkins M, Jones MD, Karran P.** 1986. Site-specific mutagenesis *in vivo* by single methylated or deaminated purine bases. Mutat Res **162:**153–163. http://dx.doi.org/10.1016/0027-5107(86)90081-3.
7. **Saparbaev M, Laval J.** 1994. Excision of hypoxanthine from DNA containing dIMP residues by the *Escherichia coli*, yeast, rat, and human alkylpurine DNA glycosylases. Proc Natl Acad Sci U S A **91:**5873–5877. http://dx.doi.org/10.1073/pnas.91.13.5873.
8. **Zhao B, O'Brien PJ.** 2011. Kinetic mechanism for the excision of hypoxanthine by *Escherichia coli* AlkA and evidence for binding to DNA ends. Biochemistry **50:**4350–4359. http://dx.doi.org/10.1021/bi200232c.
9. **Chakravarti D, Ibeanu GC, Tano K, Mitra S.** 1991. Cloning and expression in *Escherichia coli* of a human cDNA encoding the DNA repair protein N-methylpurine-DNA glycosylase. J Biol Chem **266:**15710–15715.
10. **O'Connor TR, Laval J.** 1991. Human cDNA expressing a functional DNA glycosylase excising 3-methyladenine and 7-methylguanine. Biochem Biophys Res Commun **176:**1170–1177. http://dx.doi.org/10.1016/0006-291X(91)90408-Y.
11. **Samson L, Derfler B, Boosalis M, Call K.** 1991. Cloning and characterization of a 3-methyladenine DNA glycosylase cDNA from human cells whose gene maps to chromosome 16. Proc Natl Acad Sci U S A **88:**9127–9131. http://dx.doi.org/10.1073/pnas.88.20.9127.
12. **O'Connor TR.** 1993. Purification and characterization of human 3-methyladenine-DNA glycosylase. Nucleic Acids Res **21:**5561–5569. http://dx.doi.org/10.1093/nar/21.24.5561.
13. **Dosanjh MK, Roy R, Mitra S, Singer B.** 1994. 1, N6-ethenoadenine is preferred over 3-methyladenine as substrate by a cloned human N-methylpurine-DNA glycosylase (3-methyladenine-DNA glycosylase). Biochemistry **33:**1624–1628. http://dx.doi.org/10.1021/bi00173a002.
14. **Saparbaev M, Kleibl K, Laval J.** 1995. Escherichia coli, Saccharomyces cerevisiae, rat and human 3-methyladenine DNA glycosylases repair 1, N6-ethenoadenine when present in DNA. Nucleic Acids Res **23:**3750–3755. http://dx.doi.org/10.1093/nar/23.18.3750.
15. **Lau AY, Wyatt MD, Glassner BJ, Samson LD, Ellenberger T.** 2000. Molecular basis for discriminating between normal and damaged bases by the human alkyladenine glycosylase, AAG. Proc Natl Acad Sci U S A **97:**13573–13578. http://dx.doi.org/10.1073/pnas.97.25.13573.
16. **O'Brien PJ, Ellenberger T.** 2004. Dissecting the broad substrate specificity of human 3-methyladenine-DNA glycosylase. J Biol Chem **279:**9750–9757. http://dx.doi.org/10.1074/jbc.M312232200.
17. **Kamiya H, Miura H, Kato H, Nishimura S, Ohtsuka E.** 1992. Induction of mutation of a synthetic c-Ha-ras gene containing hypoxanthine. Cancer Res **52:**1836–1839.
18. **Gates FT, Linn S.** 1977. Endonuclease V of *Escherichia coli*. J Biol Chem **252:**1647–1653.
19. **Yao M, Hatahet Z, Melamede RJ, Kow YW.** 1994. Purification and characterization of a novel deoxyinosine-specific enzyme, deoxyinosine 3′endonuclease, from *Escherichia coli*. J Biol Chem **269:**16260–16268.
20. **He B, Qing H, Kow YW.** 2000. Deoxyxanthosine in DNA is repaired by *Escherichia coli* endonuclease V. Mutat Res **459:**109–114. http://dx.doi.org/10.1016/S0921-8777(99)00063-4.
21. **Cao W.** 2013. Endonuclease V: an unusual enzyme for repair of DNA deamination. Cell Mol Life Sci **70:**3145–3156. http://dx.doi.org/10.1007/s00018-012-1222-z.
22. **Lopez-Olmos K, Hernández MP, Contreras-Garduño JA, Robleto EA, Setlow P, Yasbin RE, Pedraza-Reyes M.** 2012. Roles of endonuclease V, uracil-DNA glycosylase, and mismatch repair in *Bacillus subtilis* DNA base-deamination-induced mutagenesis. J Bacteriol **194:**243–252. http://dx.doi.org/10.1128/JB.06082-11.
23. **Aamodt RM, Falnes PØ, Johansen RF, Seeberg E, Bjørås M.** 2004. The *Bacillus subtilis* counterpart of the mammalian 3-methyladenine DNA glycosylase has hypoxanthine and 1,N^6-ethenoadenine as preferred substrates. J Biol Chem **279:**13601–13606. http://dx.doi.org/10.1074/jbc.M314277200.
24. **Bagyan I, Casillas-Martinez L, Setlow P.** 1998. The *katX* gene, which codes for the catalase in spores of *Bacillus subtilis*, is a forespore-specific gene controlled by σ^F, and KatX is essential for hydrogen peroxide resistance of the germinating spore. J Bacteriol **180:**2057–2062.
25. **Höper D, Völker U, Hecker M.** 2005. Comprehensive characterization of the contribution of individual SigB-dependent general stress genes to stress resistance of *Bacillus subtilis*. J Bacteriol **187:**2810–2826. http://dx.doi.org/10.1128/JB.187.8.2810-2826.2005.
26. **Reder A, Höper D, Gerth U, Hecker M.** 2012. Contributions of individual σ^B-dependent general stress genes to oxidative stress resistance of *Bacillus subtilis*. J Bacteriol **194:**3601–3610. http://dx.doi.org/10.1128/JB.00528-12.
27. **Sambrook J, Fritsch EF, Maniatis T.** 1989. Molecular cloning: a laboratory manual, 2nd ed. Cold Spring Harbor Laboratory, Cold Spring Harbor, NY.
28. **Vagner V, Dervyn E, Ehrlich SD.** 1998. A vector for systematic gene inactivation in *Bacillus subtilis*. Microbiology **144:**3097–3104. http://dx.doi.org/10.1099/00221287-144-11-3097.
29. **Barajas-Ornelas RC, Ramirez-Guadiana FH, Juarez-Godinez R, Ayala-Garcia VM, Robleto EA, Yasbin RE, Pedraza-Reyes M.** 2014. Error-prone processing of apurinic/apyrimidinic (AP) sites by PolX underlies a novel mechanism that promotes adaptive mutagenesis in *Bacillus subtilis*. J Bacteriol **196:**3012–3022. http://dx.doi.org/10.1128/JB.01681-14.
30. **Sun DX, Stragier P, Setlow P.** 1989. Identification of a new sigma-factor involved in compartmentalized gene expression during sporulation of *Bacillus subtilis*. Genes Dev **3:**141–149. http://dx.doi.org/10.1101/gad.3.2.141.
31. **Feucht A, Lewis PJ.** 2001. Improved plasmid vectors for the production of multiple fluorescent protein fusions in *Bacillus subtilis*. Gene **264:**289–297. http://dx.doi.org/10.1016/S0378-1119(01)00338-9.
32. **Schaeffer P, Millet J, Aubert JP.** 1965. Catabolic repression of bacterial sporulation. Proc Natl Acad Sci U S A **54:**704–711. http://dx.doi.org/10.1073/pnas.54.3.704.
33. **Nicholson WL, Setlow P.** 1990. Sporulation, germination and outgrowth, p 391–450. *In* Harwood CR, Cutting SM (ed), Molecular biological methods for *Bacillus*. John Wiley & Sons, Sussex, England.
34. **Miller JH.** 1972. Experiments in molecular genetics. Cold Spring Harbor Laboratory Press, Cold Spring Harbor, NY.
35. **Mason JM, Fajardo-Cavazos P, Setlow P.** 1988. Levels of mRNAs which code for small, acid-soluble spore proteins and their LacZ gene fusions in sporulating cells of *Bacillus subtilis*. Nucleic Acids Res **16:**6567–6583. http://dx.doi.org/10.1093/nar/16.14.6567.
36. **Tennen R, Setlow B, Davis KL, Loshon CA, Setlow P.** 2000. Mechanisms of killing of spores of *Bacillus subtilis* by iodine, glutaraldehyde and nitrous acid. J Appl Microbiol **89:**330–338. http://dx.doi.org/10.1046/j.1365-2672.2000.01114.x.
37. **Steil L, Serrano M, Henriques AO, Völker U.** 2005. Genome-wide analysis of temporally regulated and compartment-specific gene expression in sporulating cells of *Bacillus subtilis*. Microbiology **151:**399–420. http://dx.doi.org/10.1099/mic.0.27493-0.
38. **Wang ST, Setlow B, Conlon EM, Lyond JL, Imamura D, Sato T, Setlow P, Losick R, Eichenberger P.** 2006. The forespore line of gene expression in *Bacillus subtilis*. J Mol Biol **358:**16–37. http://dx.doi.org/10.1016/j.jmb.2006.01.059.
39. **Haldenwang WG.** 1995. The sigma factors of *Bacillus subtilis*. Microbiol Rev **59:**1–30.
40. **Shapiro R, Pohl SH.** 1968. The reaction of ribonucleosides with nitrous acid. Side products and kinetics. Biochemistry **7:**448–455.
41. **Choi PS, Naal Z, Moore C, Casado-Rivera E, Abruna HD, Helmann JD, Shapleigh JP.** 2006. Assessing the impact of denitrifier-produced nitric oxide on other bacteria. Appl Environ Microbiol **72:**2200–2205. http://dx.doi.org/10.1128/AEM.72.3.2200-2205.2006.
42. **Fang FC.** 2004. Antimicrobial reactive oxygen and nitrogen species: concepts and controversies. Nat Rev Microbiol **2:**820–832. http://dx.doi.org/10.1038/nrmicro1004.
43. **Morohoshi F, Hayashi K, Munkata N.** 1993. *Bacillus subtilis alkA* gene encoding inducible 3-methyladenine DNA glycosylase is adjacent to the *ada* operon. J Bacteriol **175:**6010–6017.
44. **Keijser BJ, Ter Beek A, Rauwerda H, Schuren F, Montijn R, van der Spek H, Brul S.** 2007. Analysis of temporal gene expression during *Bacillus subtilis* spore germination and outgrowth. J Bacteriol **189:**3624–3634. http://dx.doi.org/10.1128/JB.01736-06.
45. **Pedraza-Reyes M, Gutiérrez-Corona F, Nicholson WL.** 1994. Temporal regulation and forespore-specific expression of the spore photoproduct

lyase gene by sigma-G RNA polymerase during *Bacillus subtilis* sporulation. J Bacteriol **176:**3983–3991.

46. **Ramírez-Guadiana FH, Barraza-Salas M, Ramírez-Ramírez N, Ortiz-Cortés M, Setlow P, Pedraza-Reyes M.** 2012. Alternative excision repair of ultraviolet B- and C-induced DNA damage in dormant and developing spores of *Bacillus subtilis*. J Bacteriol **194:**6096–6104. http://dx.doi.org/10.1128/JB.01340-12.
47. **Ramírez-Guadiana FH, Barajas-Ornelas RC, Ayala-García VM, Yasbin RE, Robleto E, Pedraza-Reyes M.** 2013. Transcriptional coupling of DNA repair in sporulating *Bacillus subtilis* cells. Mol Microbiol **90:**1088–1099. http://dx.doi.org/10.1111/mmi.12417.
48. **Ramírez-Guadiana FH, Barajas-Ornelas RC, Corona-Bautista SU, Setlow P, Pedraza-Reyes M.** 2016. The RecA-dependent SOS response is active and required for processing of DNA damage during *Bacillus subtilis* sporulation. PLoS One **11:**e0150348. http://dx.doi.org/10.1371/journal.pone.0150348.
49. **Nicolas P, Mäder U, Dervyn E, Rochat T, Leduc A, Pigeonneau N, Bidnenko E, Marchadier E, Hoebeke M, Aymerich S, Becher D, Bisicchia P, Botella E, Delumeau O, Doherty G, Denham E, Fogg M, Fromion V, Goelzer A, Hansen A, Härtig E, Harwood C, Homuth G, Jarmer H, Jules M, Klipp E, Le Chat L, Lecointe F, Lewis P, Liebermeister W, March A, Mars R, Nannapaneni P, Noone D, Pohl S, Rinn B, Rügheimer F, Sappa P, Samson F, Schaffer M, Schwikowski B, Steil L, Stülke J, Wiegert T, Devine K, Wilkinson A, van Dijl J, Hecker M, Völker U, Bessières P, Noirot P.** 2012. Condition-dependent transcriptome reveals high-level regulatory architecture in *Bacillus subtilis*. Science **335:**1103–1106. http://dx.doi.org/10.1126/science.1206848.
50. **Morohoshi F, Munakata N.** 1983. Adaptive response to simple alkylating agents in *Bacillus subtilis* cells. Mutat Res **110:**23–37. http://dx.doi.org/10.1016/0027-5107(83)90015-5.
51. **Morohoshi F, Munakata N.** 1985. *Bacillus subtilis* mutants deficient in the adaptive response to simple alkylating agents. J Bacteriol **161:**825–830.
52. **Morohoshi F, Munakata N.** 1995. Diverse capacities for the adaptive response to DNA alkylation in *Bacillus* species and strains. Mutat Res **337:**97–110. http://dx.doi.org/10.1016/0921-8777(95)00013-A.
53. **Morohoshi F, Hayashi K, Munakata N.** 1990. *Bacillus subtilis ada* operon encodes two DNA alkyltransferases. Nucleic Acids Res **18:**5473–5480. http://dx.doi.org/10.1093/nar/18.18.5473.
54. **Singer B, Grunberger D.** 1983. Molecular biology of mutagens and carcinogens, p 45–96. Plenum Press, New York, NY.
55. **Mielecki D, Wrzesiński M, Grzesiuk E.** 2015. Inducible repair of alkylated DNA in microorganisms. Mutat Res **763:**294–305. http://dx.doi.org/10.1016/j.mrrev.2014.12.001.
56. **Setlow B, Tautvydas KJ, Setlow P.** 1998. Small, acid-soluble spore proteins of the α/β type do not protect the DNA in *Bacillus subtilis* spores against base alkylation. Appl Environ Microbiol **64:**1958–1962.